

Assessing isomeric structures of pincer-ligated ruthenium and osmium polyhydrides using density functional calculations

LORI ANNE WATSON and KENNETH G. CAULTON*

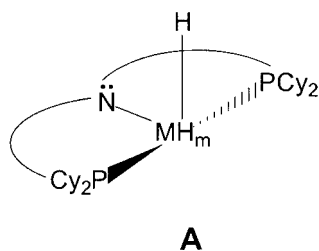
Department of Chemistry, Indiana University, Bloomington, IN 47405-7102, USA

(Received 7 February 2001; accepted 27 March 2001)

DFT calculations on a $[\text{N}(\text{SiH}_2\text{CH}_2\text{PH}_2)_2]\text{MH}_3$ model ($\text{M} = \text{Ru}$ and Os) of experimentally known compounds show that the three H have different bonding modes for Ru ($\text{H} + \text{H}_2$) and for Os (three independent H). Calculation shows that the $\text{Ru}(\text{H})(\text{H}_2)$ compound adds H_2 to give an $\text{RuH}(\text{H}_2)_2$ substructure; the $\text{Os}(\text{H})_3$ species adds H_2 to give the $\text{Os}(\text{H})_3(\text{H}_2)$ substructure. The impact of these intramolecular redox processes on bond lengths is discussed, as are attempts to provide an improved computational model of $\text{P}(\text{alkyl})_n$ without the introduction of additional alkyl atoms.

1. Introduction

We are in the process of synthesis and characterization of seemingly analogous compounds $[\text{N}(\text{SiMe}_2\text{CH}_2\text{PCy}_2)_2]\text{MH}_n$, where $\text{Cy} = \text{cyclohexyl}$, $\text{M} = \text{Ru}$ and Os and $n = 3$ and 5 . These molecules are of interest for their potential to hydrogenate small molecule C/E double or triple bonds (e.g. olefins, alkynes, ketones). Our earlier studies [1] have established the ability of a lone pair on the α atom of a ligand, such as halide or alkoxides, to donate to an otherwise empty orbital on the metal. The molecules under study here have an amide nitrogen (A), and thus exemplify a case where



only one lone pair is involved and can provide temporary stability to an unsaturated, and thus highly reactive, species. We have already synthesized $[\text{N}(\text{SiMe}_2\text{CH}_2\text{PCy}_2)_2]\text{RuH}_3$, and we are interested in *anticipating* how the osmium analogue might compare, prior to carrying out the experimental study.

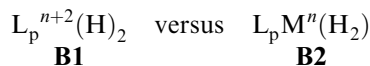
Transition metal polyhydride complexes, species L_nMH_m , where $m \geq 2$, remain challenging to characterize structurally. It was shown [2] that two H ligands

can have a bond between them; intact (even if 'stretched') H_2 can bind to a metal. One parameter difficult to establish *experimentally* is the H–H distance, as well as the judgment as to whether that distance (e.g. as long as 1.3 Å; cf. 0.72 Å in free H_2) indicates *some* H–H bonding, or none at all. In particular, neither vibrational spectroscopy nor X-ray diffraction answers the question reliably. A second difficulty in establishing the equivalence or non-equivalence of H ligands in a polyhydride species is the fact that the barrier to H site exchange is normally very low, and thus NMR spectra often fail to reflect the true lower symmetry of the ground state geometric structure; rapid hydride site exchange leads to a time-averaged single signal even when the H ligands do not occupy symmetry-related positions. This is precisely the situation for $[\text{N}(\text{SiMe}_2\text{CH}_2\text{PCy}_2)_2]\text{RuH}_3$, where ^1H NMR studies are confused by dynamically-averaged spectra at the lowest available temperature.

The evaluation of these polyhydride complexes, and their assignment as $(\text{H})_2$ or (H_2) species, is also among the most challenging computational problems. Owing to the flatness of the dihydrogen–dihydride potential energy surface in many cases, small errors introduced in the calculations of energies for these species can have large effects on the optimized geometries of the studied complexes [3]. Changes in the computational model or method employed likewise can change the optimized structure (compare, for example, the use of MP2 versus BLYP—the former which overestimates and the latter which underestimates the dihydrogen–metal interaction) [4]. However, the ability of available density functional theory (DFT) software [5] to optimize geometry of a given chemical formula, and thus to evaluate the relative energies of suggested alternative struc-

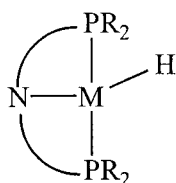
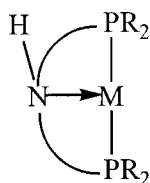
* Author for correspondence. e-mail: caulton@indiana.edu

tures, can have special importance when used in conjunction with experimental data. For the particular case at hand, 'structures' include not only geometric isomers (e.g. *cis* versus *trans*), but also the *redox* isomeric alternatives **B1** and **B2**.



Computational studies have added to experimental understanding of a variety of Ru and Os polyhydride species, in particular the $MXYL'(PR_3)_2$ class of compounds. In general, both experimental and computational studies of polyhydride complexes of Ru have shown that in these cases, a dihydrogen (H_2) structure is preferred over the alternative dihydride (H_2) redox isomer [6]; the trend is reversed for the more reducing Os metal centre [7].

Much of the previous computational work with Ru and Os complexes has focused on non-chelating, bisphosphine complexes; in the present work we seek to examine computationally the effect of a pincer ligand on the nature of group 8 polyhydride complexes. The group of Fryzuk has pioneered [8] the ligand class $(R_2PCH_2SiMe_2)_2N^-$, which is attractive to us because it provides an opportunity to incorporate steric bulk (via R) and an anionic, π -donor ligand (amide N) in a ruthenium (and osmium) complex analogous to the widely-studied, 16-valence electron $RuXYL'(PR_3)_2$. We will also consider other structures for the (PNP)MH₃ type species; as the work of Fryzuk has shown, an *additional* alternative structure for a hydride complex containing an amide ligand **C** is the amine isomer, **D**.

**C****D**

It will also be shown that the nature of each complex (i.e. dihydrogen or dihydride ligands) is stable with respect to the computational model chosen.

2. Computational model

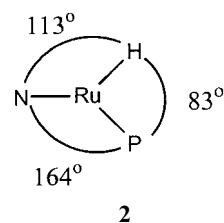
The computational model chosen for the $N[SiMe_2-CH_2P(cyclohexyl)_2]_2^{-1}$ ligand is $N[SiH_2CH_2PH_2]_2^{-1}$. This should faithfully represent the geometric (ring) constraint within a tridentate ligand, as well as the electron withdrawing character of two silicons on N. Past studies of PH_3 as a model of $P(alkyl)_3$ have shown that $\angle H-P-H$

is smaller than $\angle C-P-C$. This significantly influences the hybridization at phosphorus, and thus the electron donor power of that phosphorus atom. Koren and Davidson [9] have suggested that one way to compensate for this PH_3 defect (versus $P(alkyl)_3$) and to better model $P(alkyl)_3$, may be to constrain all $H-P-H$ angles in PH_3 to the $C-P-C$ values in a relevant $P(alkyl)_3$. We will investigate here expanding the *single* $H-P-H$ angle in each arm of $N(SiH_2CH_2PH_2)_2^{-1}$ from its refined value of $\sim 97^\circ$ from DFT calculations to the $C-P-C$ value of 101.9° in the experimentally-characterized $N[SiMe_2-CH_2P(cyclohexyl)_2]RuH(PCy_3)$ [10]. These results will be further compared here with geometry optimized methyl-substituted PNP complexes, using $N(SiH_2CH_2-PMe_2)_2^{-1}$ as the model ligand.

3. Results and discussion

3.1. (PNP)RuHL

The structure of $[N(SiMe_2CH_2PCy_2)_2]RuH(PCy_3)$ (**1**) has been determined by X-ray diffraction [10]. Consistent with the structure determination problem laid out in §1 of this paper, the hydride ligand was not detected in experimental X-ray-derived electron density maps using $-160^\circ C$ data. Geometry optimization of this compound with DFT calculations was undertaken to locate the hydride as well as evaluate the computational model chosen (namely, $N[SiH_2CH_2PH_2]_2^{-1}$). The geometry optimized structure (figure 1) for the model species $[N(SiH_2CH_2PH_2)_2]RuH(PH_3)$ is compared to the experimental data in table 1. The agreement is satisfactory, with a 0.03 \AA or less deviation in most bond distances. The hydride ligand location from the computational study (**2**) shows it to have neither a

**2**

square-pyramidal ($\angle N-Ru-H$ too large), nor a trigonal bipyramidal structure ($\angle H-Ru-P$ too small), and the result, with an experimental $N-Ru-P$ angle of 158.5° , can be best described as the Y geometry rationalized by orbital symmetry arguments [11] as yielding optimal N (lone pair) \rightarrow Ru π -donation.

3.2. (PNP)RuH_n

3.2.1. Sensitivity to the functional employed

For both $n = 3$ (**3**) and $n = 5$ (**4**), comparison of the ruthenium structures for (a) B3PW91 and (b) B3LYP

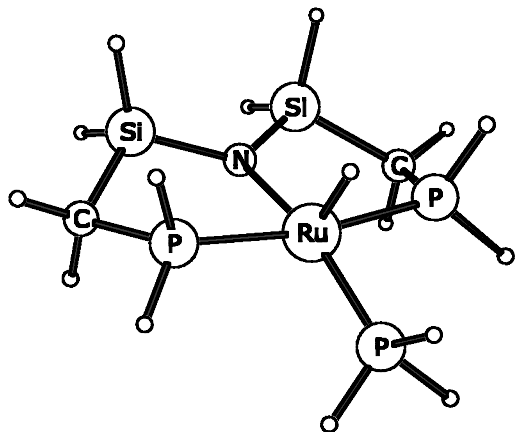


Figure 1. Geometry optimized structure of (PNP)RuH(PH₃) (see table 1 for parameters).

Table 1. Comparison of calculated and experimental structure of (PNP)RuH(PR₃).

Species Origin	(PNP)RuH(PH ₃) Calculation	(PNP)RuH(PCy ₃) Experimental
Structure #	2	1
Functional	B3PW91	N/A—averaged
Ru–N	2.118	2.15
N–Si	1.734	1.71
Si–C	1.876	1.87
C–P	1.850	1.83
P–Ru	2.326	2.37
Ru–PR ₃	2.275	2.24
Ru–H	1.562	N/A
N–Ru–H	113.0	N/A
N–Ru–PR ₃	164.2	158.5

functionals shows (table 2) differences of 0.005 to 0.04 Å. In no case was the nature of the compound (i.e. which redox isomer was located as an energy minimum) dependent on the particular functional employed. While it is important to establish these differences, rarely will an experimentalist rely on values to within 0.04 Å, except in a *comparative* computational study, where trends should then be better represented than are absolute values.

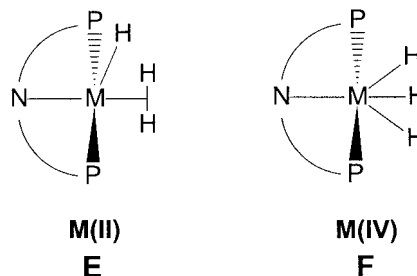
3.2.2. Influence of the number of H ligands on the P₂Si₂NM substructure

Structural parameter changes on going to (PNP)MH₅ from (PNP)MH₃ are instructive (figure 2). Bond length changes are due to contributions from higher coordination number (lengthening the distances), and from electronic effects. The latter include a decrease in N→M π-donation in the (PNP)MH₅ complex due to the 18-electron count (versus 16 e⁻ for the unsaturated

(PNP)RuH₃ species). The M–P distances should vary to a lesser extent as there are no π effects for the phosphines; these M–P bonds lengthen by only 0.01–0.02 Å for both metals and for either functional. These changes are very small compared to the N–M lengthening on going to (PNP)MH₅, which is (table 3) 0.09 Å for Ru and 0.14 Å for the more reducing Os. The suggestion that N–M multiple bond character is diminished in forming (PNP)MH₅ from (PNP)MH₃ is further supported by the (modest) pyramidalization at N in the saturated H₅ species; the sum of angles at N decreases from 358.3° to 354.5° for Ru and from 359.7° to 354.3° for Os. Finally, the N–Si bond shortens by 0.018–0.032 Å on going to the MH₅ species from the MH₃, consistent with some modest increase in N (lone pair) → Si π donation when this lone pair is no longer donating to the metal.

3.2.3. Redox isomer preferences for (PNP)MH₃ species

An exploration of the potential energy surface shows only one energy minimum for each (PNP)MH₃ species. For M = Ru, this is the hydride/dihydrogen form **E**, while for M = Os, this is the trihydride form **F**. No



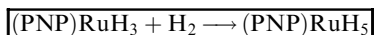
Ru(H)₃ minimum is found and no OsH(H₂) minimum is found. This preference for *different* structures is consistent with the greater reducing power of Os (versus Ru) leading to Os(IV) versus Ru(II) ground states. Adoption of *different* ground state structures is still a remarkable ‘violation’ of traditional periodic table trends: identical structures for isoelectronic species. Moreover, while it is a truism that Os is more reducing than Ru, the fact that Ru and Os lie on *opposite* sides of the (H)₂ versus (H₂) forms could not have been predicted. This ability to distinguish the nature of the H ligands is a particular strength of the computational approach. Such an analysis can often not be carried out experimentally; for example, in this case, the hydride resonances at δ = 15.03 ppm in [N(SiMe₂CH₂PCy₂)₂]RuH₃ could not be decoalesced even at low temperature.

The Ru species is calculated to have a H–H distance of 0.95 Å (table 4, figure 2), lengthened considerably from the value calculated in free H₂ (0.74 Å), due to

Table 2. Comparison of B3PW91 and B3LYP optimized geometries and energies.

Species	(PNP)RuH ₃	(PNP)RuH ₃	(PNP)RuH ₅	(PNP)RuH ₅
Structure #	3	3	4	4
Functional	B3PW91	B3LYP	B3PW91	B3LYP
H1-H2	1.806	1.848	1.950	1.979
H2-H3	0.955	0.913	0.918	0.886
H4-H5	N/A	N/A	0.808	0.791
Ru-H1	1.560	1.567	1.585	1.587
Ru-H2	1.676	1.701	1.674	1.698
Ru-H3	1.665	1.690	1.700	1.725
Ru-H4	N/A	N/A	1.885	1.937
Ru-H5	N/A	N/A	1.885	1.937
A-P-A (a = C, H)	96.9	97.0	97.1	97.2
Ru-N:	2.087	2.111	2.178	2.203
N-Si:	1.738	1.737	1.720	1.720
Ru-P:	2.330	2.356	2.340	2.366

Calculated energies for the reaction:



B3PW91 without ZPE: -3.92 kcal mol⁻¹

B3PW91 with ZPE: 0.38 kcal mol⁻¹

B3PW91 with BSSE: -3.08 kcal mol⁻¹

B3LYP without ZPE: -1.99 kcal mol⁻¹

B3LYP with ZPE: 1.96 kcal mol⁻¹

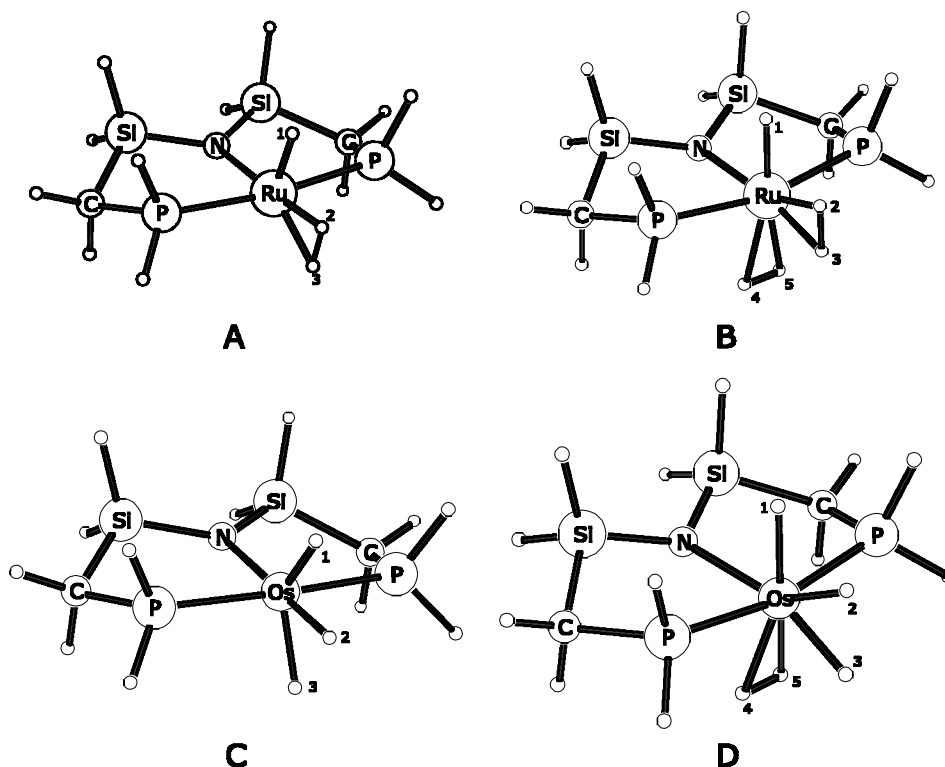
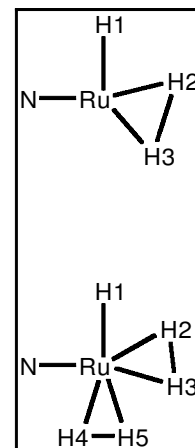


Figure 2. Geometry optimized structure of (PNP)M(H)_n (see tables 4 and 5 for parameters).

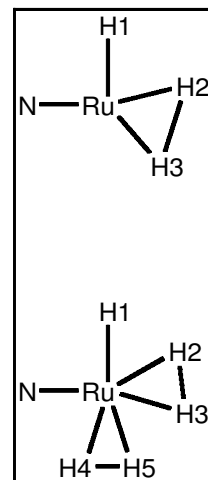
Table 3. Comparison of bond lengths and pyramidization, based on B3PW91 functionals.

Species Structure #	(PNP)RuH(PH ₃) 2	(PNP)RuH ₃ 3	(PNP)RuH ₅ 4	(PNP)OsH ₃ 5	(PNP)OsH ₅ 6
M–N	2.118	2.087	2.178	2.062	2.205
N–Si	1.733	1.738	1.720	1.755	1.723
M–P	2.326	2.330	2.340	2.316	2.337
Sum of angles around N	352.8	358.3	354.5	359.7	354.3

Table 4. Comparison of structural parameters of (PNP)RuH_n (constrained and unconstrained angle calculations; all are with the B3PW91 functional).

Species	(PNP)RuH ₃	(PNP-Me)RuH ₃	(PNP-CA)RuH ₃	(PNP-CA ₂)RuH ₅
H1–H2	1.806	1.789	1.805	1.803
H2–H3	0.955	0.988	0.958	0.964
H4–H5	N/A	N/A	N/A	N/A
Ru–H1	1.560	1.563	1.561	1.561
Ru–H2	1.676	1.664	1.675	1.673
Ru–H3	1.665	1.652	1.664	1.661
Ru–H4	N/A	N/A	N/A	N/A
Ru–H5	N/A	N/A	N/A	N/A
A–P–A (a=C, H)	96.9	101.5	101.9	113.0
Ru–N:	2.087	2.088	2.088	2.088
N–Si:	1.738	1.735	1.737	1.735
Ru–P:	2.330	2.344	2.331	2.341

Species	(PNP)RuH ₅	(PNP-Me)RuH ₅	(PNP-CA)RuH ₅
H1–H2	1.950	1.942	1.949
H2–H3	0.918	0.933	0.920
H4–H5	0.808	0.817	0.809
Ru–H1	1.585	1.590	1.586
Ru–H2	1.674	1.665	1.673
Ru–H3	1.700	1.692	1.699
Ru–H4	1.885	1.859	1.882
Ru–H5	1.885	1.859	1.882
A–P–A (a=C, H)	97.1	101.6	101.9
Ru–N:	2.178	2.179	2.178
N–Si:	1.720	1.717	1.720
Ru–P:	2.340	2.355	2.344



back donation into $\sigma^*(\text{H}-\text{H})$ enhanced by the π -donor amide ligand *trans* to itself. RuH bond lengths to H₂ hydrogens are $\sim 0.1 \text{ \AA}$ longer than to Ru–H (1.66 \AA versus 1.56 \AA), consistent with neutron diffraction structural data on MH(H₂) compounds [12].

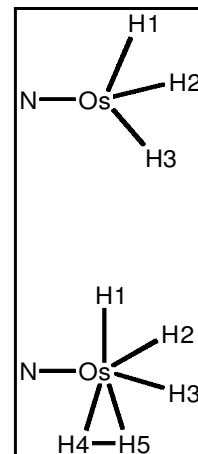
Optimization of the Os species shows *no* H–H bonding, with the *cis*-H–Os–H angles 57.5° and the (non-bonded) H–H separations at 1.55 \AA (table 5, figure 2). The cause of this small $\angle \text{H}-\text{M}-\text{H}$ has been traced earlier [13] to (a) the avoidance of two hydrides being mutually *trans* and (b) the rehybridization of an Os d_π orbital to make it π -bond more effectively with the amide nitrogen lone pair.

3.2.4. Redox isomer preferences for (PNP)MH₅ species

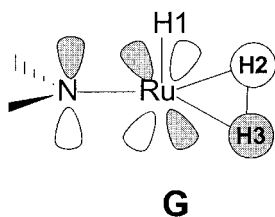
Calculations on the MH₅ species also reveal metal-dependent differences. For Ru, the ground state structure is the H(H₂)₂ isomer (table 4), and the H₂ *trans* to N has a longer H–H distance (0.92 \AA) than that *trans* to hydride (0.80 \AA), consistent with differential back donation into each of the $\sigma^*(\text{H}-\text{H})$ caused by the *trans* ligand, H or N. The Ru–H(hydride) distance (1.58 \AA) is shorter than those to H₂, and a shorter H–H distance (to H4 and H5), 0.80 \AA , correlates with a longer Ru–H distance, 1.88 \AA (cf. $\sim 1.68 \text{ \AA}$ to H2 and H3). Increased back donation to H₂ shortens those Ru–H distances.

Table 5. Comparison of structural parameters of (PNP)OsH_n (constrained and unconstrained angle calculations; all are with the B3PW91 functional).

Species	(PNP)OsH ₃	(PNP-Me)OsH ₃	(PNP-CA)OsH ₃	
H1–H2	1.555	1.598	1.588	
H2–H3	1.585	1.574	1.556	
H4–H5	N/A	N/A	N/A	
Os–H1	1.603	1.600	1.568	
Os–H2	1.653	1.655	1.653	
Os–H3	1.598	1.603	1.603	
Os–H4	N/A	N/A	N/A	
Os–H5	N/A	N/A	N/A	
A–P–A (a=C, H)	97.3	101.8	101.9	
Os–N:	2.062	2.050	2.062	
N–Si:	1.755	1.753	1.754	
Os–P:	2.316	2.330	2.319	
Species	(PNP)OsH ₃	(PNP-Me)OsH ₃	(PNP-CA)OsH ₃	(PNP-CA ₂)OsH ₅
H1–H2	1.758	1.754	1.749	1.748
H2–H3	1.492	1.514	1.495	1.506
H4–H5	0.862	0.884	0.865	0.872
Os–H1	1.623	1.628	1.623	1.625
Os–H2	1.609	1.611	1.610	1.610
Os–H3	1.633	1.623	1.633	1.633
Os–H4	1.812	1.787	1.808	1.800
Os–H5	1.812	1.787	1.808	1.800
A–P–A (a=C, H)	97.9	102.2	101.9	113.0
Os–N:	2.205	2.205	2.206	2.206
N–Si:	1.723	1.720	1.722	1.721
Os–P:	2.337	2.352	2.340	2.348



The two H₂ molecules are orthogonal, which is a symptom of their interacting with *different* d_π orbitals for back donation. Here, as in (PNP)RuH(H₂), the H₂ *trans* to amide adopts a rotational conformation which allows it to π-accept from the metal d orbital which is destabilized by interaction with the amide nitrogen p_π orbital (G). This rotational conformation also minimizes

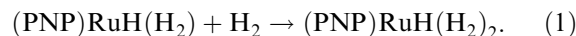


steric contact of H2–H3 with the bulky phosphine, and benefits from a stabilizing ‘*cis*-effect’ [14] interaction with H1. The orientation and H–H bond distances in this (PNP)RuH₅ species are nearly identical with the optimized geometry at Ru(PH₃)₂ClH(H₂)₂, which has H–H distances of 0.95 Å and 0.82 Å (*cis* and *trans* to the hydride, respectively) [6].

The ground state structure for (PNP)OsH₅ is found (table 5) to be (H)₃(H₂), unlike the Ru congener. This is the ‘obvious’ product of addition of H₂ to the Os(H)₃ species. In sum, the reducing power of osmium is not sufficient to make Os(VI), Os(H)₅, the ground state structure. In this case, Ru and Os exist as different redox isomers.

4. Binding energies

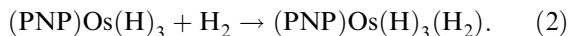
The reaction energy for binding H₂ to (PNP)MH₃ (equation (1)) was calculated for each M.



The value for Ru without ZPE correction is –3.9 kcal mol^{–1} at B3PW91; with ZPE correction included, this value becomes +0.4. Analysis of the zero point energy of each contributing species shows the relatively large ZPE correction to ΔE can be attributed to the ZPE for (PNP)RuH(H₂) due to the ‘soft’ vibrational nature of these Ru–H and H–H bonds. With the ZPE correction included, this system is essentially non-bonding. The entropy change will also make H₂ binding even less favourable, except at low temperature. These

results are consistent with the experimental observation of a major mole fraction of $[\text{N}(\text{SiMe}_2\text{CH}_2\text{PCy}_2)_2]\text{RuH}_5$ only at -90°C under 1 atm H_2 . This low affinity for H_2 also explains why unsaturated $[\text{N}(\text{SiMe}_2\text{CH}_2\text{PCy}_2)_2]\text{-RuH}(\text{H}_2)$ is experimentally obtained during solvent removal in vacuum.

Osmium is generally more reluctant to be unsaturated; hence, the reaction energy for equation (2) might be expected to be exothermic.



In fact, the calculated value (without ZPE) is $-4.2 \text{ kcal mol}^{-1}$; with ZPE correction this value becomes $0.4 \text{ kcal mol}^{-1}$, with the larger than usual ZPE correction due again to 'soft' Os–H and H–H vibrations. There is thus *no* real significant metal effect on these energetics.

BSSE corrections of $+0.8$ and $+0.9 \text{ kcal mol}^{-1}$ to ΔE (without ZPE) for Ru and Os respectively, yield BSSE-corrected ΔE of -3.1 and $-3.3 \text{ kcal mol}^{-1}$ for equations (1) and (2). This correction does not yield different qualitative results than already discussed.

5. Alternative models of phosphorus substituents

We have examined the sensitivity of the calculated structures to one aspect of the model chosen for the molecular composition: the use of H, rather than alkyl, on phosphorus. While modelling $\text{P}(\text{alkyl})_3$ by PH_3 has been conventional, the fact that the H–P–H angle in PH_3 is significantly smaller than that in $\text{P}(\text{alkyl})_3$ is cause for concern. In particular, the implied change in the composition (and energy) of the lone pair in PR_3 as the angle R–P–R changes could significantly influence metal–ligand structural features. In a thesis, Koren has suggested [9] an intriguing economical compromise: calculating PR_3 with a PH_3 model, but with $\angle\text{H–P–H}$ constrained to the experimental value of $\angle\text{C–P–C}$ ('CA', for constrained angle). This change can thus be used for checking the stability of the calculations with respect to the model employed.

To explore this proposal, and in an $(\text{alkyl})\text{PH}_2$ context, we have assessed otherwise comparable calculations of several species of interest here. We anticipate that the H–H distance in a dihydrogen ligand, because it is in general strongly influenced by changes in ligand substituents, will sensitively reflect the consequences of alternative modelling of the phosphine substituents. Bending $\angle\text{H–M–H}$ is generally a very 'soft' parameter and this angle should thus be sensitive to the model chosen. In particular, better donation by the phosphine should be reflected in greater electron transfer into the $\sigma^*(\text{H–H})$ orbital, and thus lengthening of the H–H distance in any dihydrogen ligand. A useful alternative criterion of model quality, the relative energy of

$\text{M}(\text{H})_2$ and $\text{M}(\text{H}_2)$ redox isomers, is not possible here since in both the Ru and Os case, one of these two is not a minimum on the PES.

Comparison (table 4) of $(\text{PNP})\text{RuH}_3$ with $(\text{PNP–CA})\text{RuH}_3$, which has both $\angle\text{H–P–H}$ angles in $\text{N}[\text{SiH}_2\text{CH}_2\text{PH}_2]_2^{-1}$ constrained to the experimental $\angle\text{C–P–C}$ value found [10] when phosphorus carries two bulky cyclohexyl substituents (101.9°), causes changes in bond distances that are negligibly small: 0.003 \AA . Even the Ru–P distance change is within this limit. The angle-dependent changes for the trihydride $\text{Os}(\text{H})_3$ species (table 5) are comparably small, as they are also for the $\text{Os}(\text{H})_3(\text{H}_2)$ species. Since a great deal of study has been made of species where the PR_2 arm contains two ^tBu groups [15], we have surveyed the experimental angles $(^t\text{Bu})\text{C–P–C}(^t\text{Bu})$ available in the literature; these are in the narrow range $110\text{--}118^\circ$. We therefore repeated our PH_2 model calculations with the H–P–H angle constrained to 113° (PNP–CA_2). This greater angle constraint also makes no significant difference in metal–ligand bonding to either the $\text{RuH}(\text{H}_2)$ species (table 4) or the $\text{Os}(\text{H})_3(\text{H}_2)$ species (table 5).

The influence of 'turning on' the electronic influence of alkyl substituents is tested by doing an unconstrained calculation with two CH_3 groups on each P, changing the model ligand to $\text{N}[\text{SiH}_2\text{CH}_2\text{PMe}_2]_2^{-1}$ (table 4). Because this model adopts essentially the same $\angle\text{C–P–C}$ as the constrained $\angle\text{H–P–H}$ (compare 101.5° to 101.9°), a comparison of these two is especially informative of electronic effects. It shows bond length changes in the $\text{RuH}(\text{H}_2)$ species of less than 0.01 \AA (which are larger than those obtained by constraining $\angle\text{H–P–H}$ to 101.9°), *except* for the H2–H3 distance which shortens by 0.03 \AA . In this case, at least, modelling with the full methyl group (but not merely with a constrained $\angle\text{H–P–H}$) gives a somewhat modified result from the unconstrained $(\text{N}(\text{SiH}_2\text{CH}_2\text{PH}_2)_2)\text{MH}_3$; however, even in the calculations done with the PNP–Me model, the structure remains stable at a $\text{RuH}(\text{H}_2)$ geometry.

The same comparisons on the saturated $(\text{PNP})\text{RuH}(\text{H}_2)_2$ species yield comparable conclusions. The largest change by constraining $\angle\text{H–P–H}$ to 101.9° is 0.003 \AA , and the supposedly sensitive H–H distances in both H_2 ligands change by even less. The constrained $\text{N}[\text{SiH}_2\text{CH}_2\text{PH}_2]_2^{-1}$ (PNP–CA) and the freely optimized $\text{N}[\text{SiH}_2\text{CH}_2\text{PMe}_2]_2^{-1}$ (PNP–Me) examples differ by less than 0.02 \AA , and the bonded H–H distances differ by less than 0.013 \AA (table 4). Qualitatively, each structure is stable to changes in the model, remaining $(\text{PNP})\text{-Ru}(\text{H})(\text{H}_2)_2$.

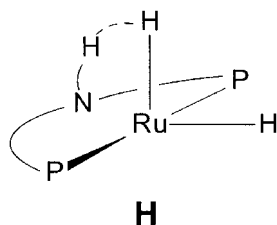
In sum, none of the above 'improvements' in model chosen have changed the calculated optimized structure to a degree that would lead an experimentalist to prefer it above the others. Alternatively said, the answer to the

question ‘dihydride or dihydrogen?’ is not altered by truer representation of the substituents in these test cases.

All three computational models of $(\text{PNP})\text{OsH}_3$ give, practically speaking, the same structure, even with a 4° increase in \angle substituent–P–substituent. In particular, no H–H distance moves significantly away from the trihydride form (i.e. no H–H bond forms) and even the Os–P distance changes by less than 0.01 Å. Similarly, no qualitative shift away from the $(\text{PNP})\text{Os}(\text{H})_3(\text{H}_2)$ structure is found, when constraining the \angle H–P–H angle or in doing an unconstrained $\text{N}[\text{SiH}_2\text{CH}_2\text{PMe}_2]_2^-$ (PNP–Me) optimization. Further constraining the \angle H–P–H value to 113.0° , the average experimental value for $(^t\text{Bu})\text{C–P–C}(^t\text{Bu})$ angles from the literature survey, show that the structural results (table 5) are remarkably robust even to this large PH_2 angle change, with no change in bond angles or distances larger than those previously cited in this section.

6. Is a structure with one H on nitrogen energetically viable?

We have also considered a structure where one H is on the nitrogen and two are on Ru; this $(\text{PNP–H})\text{Ru}(\text{H})_2$ structure represents an isomer of $(\text{PNP})\text{RuH}(\text{H}_2)$. It is well known that a dihydrogen ligand can exhibit Brønsted acid behaviour, and an amide ligand is subject to protonation (and thus an Ru–NR_2 bond is subject to protolytic *cleavage*). One additional aspect of the structure envisioned in **H** is the possibility that an amine hydrogen can be suffi-



ciently acidic that it hydrogen bonds to a hydride ligand on Ru. Searches of the PES beginning from a non-bonded N–Ru distance but with the amine proton within hydrogen bonding distance of the hydride on Ru, and also independently from a Ru-coordinated amine where the N–H vector points away from Ru, produced the same minimum, whose structure is shown in figure 3. The angles around N sum to 351.4° , indicating very little pyramidal character (table 6). Noteworthy is the fact that the N–H vector points towards the hydride H2 (but the H1–H2 distance, 2.17 Å, is too long for a

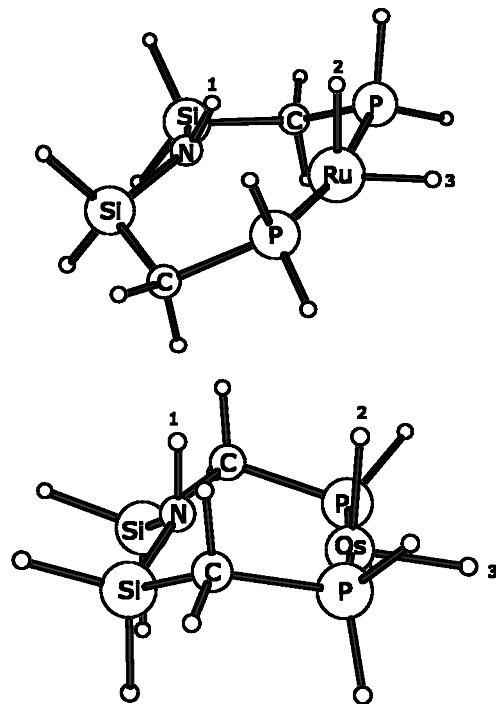


Figure 3. Geometry optimized structure of $(\text{PNP–H})\text{MH}_2$ (see table 6 for structural parameters).

Table 6. Comparison of structural parameters of $(\text{PNO–H})\text{MH}_2$, using B3PW91 functionals.

Species	$(\text{PNP–H})\text{RuH}_2$	$(\text{PNP–H})\text{OsH}_2$
H1–H2	2.170	2.465
H2–H3	2.084	2.355
M–H1	2.260	2.786
M–H2	1.564	1.590
M–H3	1.580	1.627
M–N	2.526	2.414
M–P	2.293	2.283
N–H	1.032	1.019
N–Si	1.765	1.781
H1–N–Ru	63.5	100.5
H2–Ru–H3	83.0	94.1
P–M–P	170.3	176.1
Sum of N angles:	351.4	344.7

hydrogen bond) [16], and the NH bond is oriented so that it might suggest some donation to Ru (the H1–N–Ru–H2 dihedral angle is 0.0°). However, the Ru–N distance (2.53 Å) and the Ru–H1 distance (2.26 Å) are too long to suggest significant bonding between these atoms. For example, the calculated Ru–N (amide) distances described in tables 1–5 range from 2.08 to 2.20 Å in complexes containing a well defined Ru–amide bond. For further comparison, the Rh–C distance to an agostic arene C–H in $\text{Rh}(\text{CO})[\text{C}_6\text{R}_3\text{H}(\text{CH}_2\text{PtBu}_2)_2]^+$

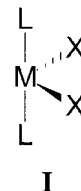
is 2.27 Å [17]. Distances from Ru, Rh and Ir to the coordinated nitrogen of $\text{HN}(\text{SiMe}_2\text{CH}_2\text{PR}_2)_2$ are in the narrow range 2.34–2.38 Å for $\text{HN}(\text{SiMe}_2\text{CH}_2\text{PR}_2)_2\text{MX}$ species [18]. All of these show hydrogen bonding to an adjacent (i.e. *syn*) halide, with a $\text{NH}\cdots\text{X}$ distance of 0.2–0.5 Å shorter than the sum of their van der Waals radii. Also suggestive of no $\text{NH}\rightarrow\text{Ru}$ donation in this calculated structure is the N–H distance, 1.03 Å, which is not significantly lengthened from that in the free amine.

To conclude, we suggest that the proximity of the N–H bond to Ru in the calculated structure is caused by ring constraints, especially the combination of a P–Ru–P angle of nearly 180° and the need of the N–H bond not to eclipse Si–H bonds on *both* of its neighbours. Significantly, when the P–M–P angle decreases (to 116.99°) in tetrahedral $\text{NiCl}_2[\text{NH}(\text{SiMe}_2\text{CH}_2\text{PPh}_2)_2]$ [19], then the less-constrained nitrogen moves much further away ($\text{N}\cdots\text{Ni} = 4.04\text{ Å}$) and there is no Ni–HN interaction ($\text{Ni–H} = 4.13\text{ Å}$). It is also significant that the DFT-calculated energy of the structure in table 6 is 11.35 kcal mol⁻¹ above the (PNP)RuH(H₂) structure. Apparently, the electron-rich character of Ru here favours a structure with a π -acid ligand (H₂) rather than two hydrides and a non-donor N–H bond.

The osmium analogue with an amine ligand provides some interesting points for comparison (figure 3). Pre-eminent among these is the fact that the (PNP–H)Os(H)₂ isomer is much more disfavoured compared to the ground state structure: 21.7 kcal mol⁻¹ higher than the trihydride, (compared to 11.4 kcal mol⁻¹ higher for (PNP–H)Ru(H)₂). The full set of structural parameters, and their differences from the Ru case, suggest some non-zero interaction in the Os case (table 6). The amine nitrogen is more pyramidal (sum of angles around N is 344.7°) than for Ru, and the Os–H bond *trans* to this N is longer (1.627 Å) than for Ru (1.580 Å). The Os \cdots H(N) distance is longer (2.786 Å) than for Ru (2.263 Å) and the N–H bond is not lengthened (1.019 Å). The Os–N distance (2.41 Å), however, is shorter than for Ru (2.53 Å) and the nitrogen lone pair points towards Os (figure 3). This Os–N distance approaches the bonded M–NH(SiMe₂CH₂PR₂)₂ distances cited above for Ru, Rh and Ir, and thus must be considered bonding. The strong *trans* influence of the hydride does not favour the formation of an Os–N bond; thus, this added interaction *fails* to lower ΔE between the (PNP)Os(H)₃ and the (PNP–H)Os(H)₂ isomeric structures. The higher energy of the amine isomer of Os compared to Ru is perhaps also partially explained by the fact that these isomers for Os have *different* metal oxidation states, which is *not* true for Ru. Structurally, however, the Ru–Os comparison shows Os to be more

Lewis acidic, interacting more strongly with the lone pair on NH(SiH₂CH₂PH₂)₂.

Fundamentally, both (PNP–H)M(H)₂ structures illustrate the previously shown preference for a 14-valence electron d⁶ ML₂(X)₂ species to have a ‘saw-horse’, or *cis*-divacant octahedral structure (I).



7. Conclusions

Density functional theory calculations provide a good method to determine selected structural and electronic trends that would be difficult or impossible to establish experimentally. One such parameter is the location, nature, and interaction of metal hydrogen ligands and the effect on such structures of changing metals or donor power of the phosphines. The geometry optimized structures for the Ru polyhydride cases showed preference for a hydride–dihydrogen and hydride–bis-dihydrogen structure for (PNP)RuH₃ and (PNP)RuH₅ complexes respectively. Calculation with a better donor phosphine, $\text{N}[\text{SiH}_2\text{CH}_2\text{PMe}_2]_2^-$ (PNP–Me), did not qualitatively change the nature of bonding of the hydrogen ligands. Consistent with experiment, the addition of H₂ to the unsaturated (PNP)RuH₃ complex is calculated to be endothermic. The (PNP)RuH(H₂)₂ complex shows a slight pyramidalization of nitrogen, the result of increasing localization of the lone pair on nitrogen.

In contrast, (PNP)OsH₃ is optimized to a trihydride structure, consistent with previous experimental observations that Os is more reducing and so in general favours polyhydride versus dihydrogen forms. Upon addition of an additional π -acidic H₂ ligand, a trihydride–dihydrogen form for (PNP)OsH₃ is seen to be preferred.

The alternative (PNP)MH₃ isomer, (PNP–H)M(H)₂, shows bond distances and degree of pyramidalization at nitrogen characteristic of a non-zero bonding interaction between the amine N and the metal centre only in (PNP–H)Os(H)₂.

These tests show the relative stability of important structural parameters to changes in the computational model. In particular, never did the discontinuous change from dihydride to dihydrogen occur on altering the model compound. The approach of widening $\angle\text{H–P–H}$ to mimic more closely the C–P–C angle in an alkyl

phosphine was shown to have no large structural consequences. This study further shows that DFT successfully captures the greater reducing power of a 5d metal compared to its 4d analogue. This is a subtle effect in reality, and it is reassuring for future applications that the results here calculate osmium to reduce H_2 to two H^- when ruthenium does not, in (PNP) MH_3 analogues. This study augurs well that the yet experimentally unstudied species (PNP)OsH₅ may indeed be (PNP)Os(H)₃(H₂). It is also consistent with the current understanding of H₂ complexes that the one H₂ ligand in (PNP)OsH₅ is *trans* to hydride; N → Os π donation is anisotropic and thus more effectively reduces any H₂ *trans* to itself.

It bears mention that our optimistic view of DFT stated here applies to structural parameters. In particular, we cannot make any comparable promise for reaction or isomerization energies, since these are not available from experiment.

8. Computational details

All calculations were performed with the Gaussian 98 package [5]. Initial geometry optimizations of (PNP)RuH_n were performed with B3PW91 [20] and B3LYP [21] functionals. No qualitative difference in the nature of the redox isomer (dihydride versus dihydrogen) was seen, and all subsequent calculations were performed at the B3PW91 level of theory. Basis sets used included LANL2DZ for Ru, Os, P, and Si, 6-31G* for C and N, and 6-31G** for all hydrogens [22]. The basis set LANL2DZ is the Los Alamos National Laboratory ECP plus a double zeta valence on Ru, Os, P and Si [23]; additional d polarization functions [24] were added to phosphorus and silicon atoms in all DFT calculations. All optimizations were performed with C₁ symmetry and minima were confirmed by analytical calculation of frequencies, which were also used to compute zero point energy corrections without scaling. BSSE corrections [25] were employed where indicated for the reaction energy of H₂ addition to MH₃ species.

The initial geometry of (PNP)RuH(PH₃) was adapted from a refined crystal structure of [N(SiMe₂CH₂PCy₂)₂]-RuH(PCy₃) with all silicon methyl and phosphorous cyclohexyl groups replaced by hydrogen. Initial geometries for the M-PNP core in the optimization of (PNP)MH_n species were taken from the optimized geometry of the Ru-PNP core of (PNP)RuH(PH₃). Several starting structures were used in each metal-H_n case corresponding to different H-H distances. Regardless of the nature of the hydrogen ligands defined in the initial geometry (hydride or dihydrogen) or their rotational conformation, each starting structure converged to that reported in tables 4 and 5. Optimizations of alter-

native MH₃ isomers (namely (PNP-H)MH₂) were started from two geometries: one in which the amine hydrogen was located perpendicular to the PNP-M plane, in a position to interact with the apical hydride, and the other in which the amine hydrogen was initially located in the plane of the PNP-M core structure. In both cases, the structures optimized to those reported in table 6.

H-P-H constrained angle calculations were performed by freezing the H-P-H angle to the desired value and optimizing the remainder of the structure by normal methods. Releasing of the constraints on selected molecules caused a return to the starting geometry, as discussed in the text.

LAW acknowledges the National Science Foundation for a predoctoral fellowship.

This paper is dedicated to Ernest R. Davidson, whose valued collaboration over the years has often clarified 'mysterious' computational results.

References

- [1] JOHNSON, T. J., FOLTING, K., STREIB, W. E., MARTIN, J. D., HUFFMAN, J. C., JACKSON, S. A., EISENSTEIN, O., and CAULTON, K. G., 1995, *Inorg. Chem.*, **34**, 488.
- [2] KUBAS, G. J., 1988, *Acc. Chem. Res.*, **21**, 120.
- [3] MASERAS, F., LLEDÓS, A., CLOT, E., and EISENSTEIN, O., 2000, *Chem. Rev.*, **100**, 601.
- [4] BYTHEWAY, I., BACSKAY, G. B., and HUSH, N. S., 1996, *J. phys. Chem.*, **100**, 6023; CLOT, R., and EISENSTEIN, O., 1998, *J. phys. Chem. A*, **102**, 3592.
- [5] FRISCH, M. J., TRUCKS, G. W., SCHLEGEL, H. B., SCUSERIA, G. E., ROBB, M. A., CHEESEMAN, J. R., ZAKRZEWSKI, V. G., MONTGOMERY, J. A., STRATMANN, R. E., BURANT, J. C., DAPPRICH, S., MILLAM, J. M., DANIELS, A. D., KUDIN, K. N., STRAIN, M. C., FARKAS, O., TOMASI, J., BARONE, V., COSSI, M., CAMMI, R., MENNUCCI, B., POMELLI, C., ADAMO, C., CLIFFORD, S., OCHTERSKI, J., PETERSSON, G. A., AYALA, P. Y., CUI, Q., MOROKUMA, K., MALICK, D. K., RABUCK, A. D., RAGHAVACHARI, K., FORESMAN, J. B., CIOSŁOWSKI, J., ORTIZ, J. V., STEFANOW, B. B., LIU, G., LIASHENKO, A., PISKORZ, P., KOMAROMI, I., GOMPERTS, R., MARTIN, R. L., FOX, D. J., KEITH, T., AL-LAHAM, M. A., PENG, C. Y., NANAYAKLARA, A., GONZALEZ, C., CHALLACOMBE, M., GILL, P. M. W., JOHNSON, B. G., CHEN, W., WONG, M. W., ANDRES, J. L., HEAD-GORDON, M., REPLOGLE, E. S., and POPLE, J. A., 1998, *Gaussian 98, Revision A.7* (Pittsburgh PA: Gaussian, Inc.).
- [6] See, for example, CHRIST, M. L., SABO-ETIENNE, S., and CHAUDRET, B., 1994, *Organometallics*, **13**, 3800; RODRIGUEZ, V., SABO-ETIENNE, S., CHAUDRET, B., THOBURN, J., ULRICH, S., LIMBACH, H. H., ECKERT, J., BARTHELAT, J. C., HUSSEIN, K., and MARSDEN, C., 1998, *J. inorg. Chem.*, **37**, 3475; ABDUR-RASHID, K., GUSEV, D. G., LOUGH, A. J., and MORRIS, R. H., 2000, *Organometallics*, **19**, 1652.
- [7] See, for example, ESTERUELAS, M. A., JEAN, Y., LLEDÓS, A., ORO, L. A., RUIZ, N., and VOLATRON, F., 1994,

- Inorg. Chem.*, **33**, 3609; GUSEV, D. G., KUHLMAN, R., SINI, G., EISENSTEIN, O., and CAULTON, K. G., 1994, *J. Am. chem. Soc.*, **116**, 2685; KUHLMAN, R., CLOT, E., STREIB, W. E., LEFORESTIER, C., EISENSTEIN, O., and CAULTON, K. G., 1997, *J. Am. chem. Soc.*, **36**, 1061; BAREA, G., ESTERUELAS, M. A., LLEDÓS, A., LOPEZ, A., ONATE, E., and TOLOSA, J. I., 1998, *Organometallics*, **17**, 4065.
- [8] FRYZUK, M. D., GIESBRECHT, G. R., JOHNSON, S. A., KICKHAM, J. E., and LOVE, J. B., 1998, *Polyhedron*, **17**, 947.
- [9] KOREN, P., 1999, PhD thesis, Indiana University.
- [10] COALTER III, J. N., HUFFMAN, J. C., and CAULTON, K. G., unpublished results.
- [11] EL IDRISSE, R.-I., EISENSTEIN, O., and JEAN, Y., 1990, *New J. Chem.*, **14**, 671; RIEHL, J.-F., JEAN, Y., EISENSTEIN, O., and PÉLISSIER, M., 1992, *Organometallics*, **11**, 729.
- [12] ECKERT T. J., JENSEN, C. M., KOETZLE, T. J., HUSEBO, T., NICOL, J., and WÜ, P., 1995, *J. Am. chem. Soc.*, **117**, 7271; BAU, R., and DRABNIS, M. H., 1997, *Inorg. Chim. Acta*, **259**, 27.
- [13] YANDULOV, D. V., HUANG, D., HUFFMAN, J. C., and CAULTON, K. G., 2000, *Inorg. Chem.*, **39**, 1919.
- [14] VAN DER SLUYS, L. S., ECKERT, J., EISENSTEIN, O., HALL, J. H., HUFFMAN, J. C., JACKSON, S. A., KOETZLE, T. F., KUBAS, G. J., VERGAMINI, P. J., and CAULTON, K. G., 1990, *J. Am. chem. Soc.*, **112**, 4831.
- [15] COOPER, A. C., STREIB, W. E., EISENSTEIN, O., and CAULTON, K. G., 1997, *J. Am. chem. Soc.*, **119**, 9069.
- [16] JEFFREY, G. A., 1997, *An Introduction to Hydrogen Bonding* (New York: Oxford University Press).
- [17] VIGALOK, A., UZAN, O., SHIMON, L., YEHOSSHA, B., MARTIN, J., and MILSTEIN, D., 1998, *J. Am. chem. Soc.*, **120**, 12539.
- [18] FRYZUK, M. D., MACNEIL, P. A., and RETTIG, S. J., 1987, *J. Am. chem. Soc.*, **109**, 2803; FRYZUK, M. D., MACNEIL, P. A., and RETTIG, S. J., 1985, *Organometallics*, **4**, 1145; FRYZUK, M. D., and MACNEIL, P. A., 1983, *Organometallics*, **2**, 682.
- [19] FRYZUK, M. D., MACNEIL, P. A., RETTIG, S. J., SECCO, A. S., and TROTTER, J., 1982, *Organometallics*, **1**, 918.
- [20] BECKE, A. D., 1988, *Phys. Rev. A*, **38**, 3098; BECKE, A. D., 1993, *J. chem. Phys.*, **98**, 1372; BECKE, A. D., 1993, *J. chem. Phys.*, **98**, 5648; PERDEW, J. P., and WANG, Y., 1991, *Phys. Rev. B*, **45**, 13244.
- [21] BECKE, A. D., 1993, *J. chem. Phys.*, **98**, 5648; LEE, C., YANG, W., and PARR, R. G., 1998, *Phys. Rev. B*, **37**, 785; STEPHENS, P. J., DEVLIN, F. J., CHABALOWSKI, C. F., and FRISCH, M. J., 1994, *J. phys. Chem.*, **98**, 11623.
- [22] HARIHARAN, P. C., and POPLE, J. A., 1973, *Theor. Chim. Acta*, **28**, 213.
- [23] HAY, P. J., and WADT, W. R., 1985, *J. chem. Phys.*, **82**, 270; WADT, W. R., and HAY, P. J., 1985, *J. chem. Phys.*, **82**, 284; HAY, P. J., and WADT, W. R., 1985, *J. chem. Phys.*, **82**, 299.
- [24] HÖLLWARTH, A., BÖHME, M., DAPPRICH, S., EHLERS, A. W., GOBBI, A., JONAS, V., KÖHLER, K. F., STEGMANN, R., VELDKAMP, A., and FRENKING, G., 1993, *Chem. Phys. Lett.*, **208**, 237.
- [25] JANSEN, H. B., and ROS, P., 1969, *Chem. Phys. Lett.*, **3**, 140.